

# Effects of Solution Processing on the Photovoltaic Response of Poly(*n*-vinyl carbazole) Films

P. S. Chung, P. H. Holloway

Department of Materials Science and Engineering, University of Florida, P.O. Box 116400, Gainesville, Florida 32611-6400

Received 30 June 2009; accepted 10 September 2009

DOI 10.1002/app.31428

Published online 18 March 2010 in Wiley InterScience (www.interscience.wiley.com).

**ABSTRACT:** The effects of solution processing on the photovoltaic response of poly(*n*-vinyl carbazole) (PVK) films were investigated. PVK films were formed by spin-casting onto glass coated with indium tin oxide (ITO) and poly(3,4-ethylenedioxythiophene) (PEDOT)–polystyrenesulfonate (PSS). Some of the PVK films were redissolved in chlorobenzene and redried in the absence or presence of an electric field. Illuminated current–voltage characteristics were measured for an ITO/PEDOT:PSS/PVK/Ca:Al device. Films spin-cast from a 50 mg/mL so-

lution, redissolved, and dried in the absence of the electric field exhibited a 26% higher charge collection efficiency than films dried in the presence of the electric field. The increased charge collection efficiency was attributed to changes in the molecular configuration of the PVK films. © 2010 Wiley Periodicals, Inc. *J Appl Polym Sci* 117: 479–485, 2010

**Key words:** atactic; conjugated polymers; luminescence; photophysics

## INTRODUCTION

Photovoltaic (PV) devices with organic active layers have been studied.<sup>1–3</sup> The simplest PV device structure consists of an active organic layer sandwiched between two electrodes. Intermediate layers may be added to aid charge transport and balance. In operation, excitons are created via light absorption and are dissociated after diffusion to a heterojunction. The energy band offsets restrict electrons and holes from crossing the junction in the same direction. The dissociated charges migrate to opposite electrodes and create an external current. Improved device performance has been realized by the addition of fullerene derivatives to the active organic layer<sup>4</sup> and through the use of highly absorbing dye molecules to promote exciton formation.<sup>5</sup> Solution processing is a potential advantage of the use of polymers for PVs. Solution-based techniques, such as spin-casting, can be done in air; thereby, costly vacuum processing and instrumentation are avoided, and the techniques are amendable to large-scale manufacturing, which is critical for significant power generation.

Despite their attractive qualities, polymer-based PVs are still in the research stage.<sup>6</sup> Compared to existing inorganic semiconductor technologies with

efficiencies of about 20–30%,<sup>7,8</sup> polymer PV device performance has only reached efficiencies of about 6%.<sup>9,10</sup> Polymers are typically amorphous and disordered; therefore, charge carriers do not move through a periodic three-dimensional atomic lattice as for inorganic semiconductors but rather are constrained by two-dimensional bonding paths and nearest-neighbor proximities. As a result, carrier mobilities are poor compared to those of inorganic semiconductors; this affects device performance.<sup>2,3</sup> The objective of this study was to investigate the effects of simple solution processing on the PV properties of single-layer poly(*n*-vinyl carbazole) (PVK) devices. To accomplish this objective, we constructed PVK-based devices and characterized them by current–voltage (*I*–*V*) measurements. Although the PV responses of these simple, single-layer PVK devices were too low for PV applications, the data showed that the charge collection efficiency ( $\eta_{CC}$ ) was increased by solution-induced molecular reconfigurations in the PVK layer.

## EXPERIMENTAL

The PVK polymer (weight-average molecular weight  $\approx$  90,000 g/mol, polydispersity index  $\approx$  2.5; see Fig. 1) was obtained from Scientific Polymer Products, Inc. (Ontario, NY), and was synthesized by free-radical polymerization. The PVK's glass-transition temperature was measured to be 215°C with differential scanning calorimetry; this was consistent with the reported value of 227°C for atactic PVK.<sup>11</sup> Syndiotactic and isotactic PVKs have glass-transition

Correspondence to: P. H. Holloway (pholl@mse.ufl.edu).

Contract grant sponsor: Army Reserve Laboratory (ARL); contract grant number: W911NF-04-200023.

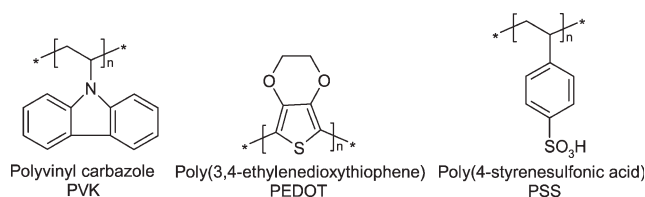


**Figure 1** Chemical structures of the polymers used in this research.

temperatures of 276 and 126°C, respectively. The PVK was dissolved in chlorobenzene at concentrations of 10, 50, and 100 mg/mL. Before use, all solutions were syringe filtered through a 0.2- $\mu\text{m}$  nylon filter from Gelman. The dispersed solution was spin-cast onto substrates at 3000 rpm for 30 s in air.

The substrates were unpolished float glass coated with 8–12  $\Omega$  per square indium tin oxide (ITO) film ( $\sim$  1200–1500 Å thick, purchased from Delta Technologies, Stillwater, MN). The ITO was patterned with Scotch tape to cover the 1  $\times$  1" substrate, except for a rectangle of about 1  $\times$  0.2" along one edge. The masked ITO was suspended over heated (30°C) aqua regia (3 : 1 mixture of HCl : HNO<sub>3</sub>) for about 5–10 min. The patterned substrates were cleaned with sonication (20 min) in Alconox-water, followed by deionized water, acetone, and isopropyl alcohol, and blow dried with nitrogen. Just before spin-casting, the substrates were exposed to an oxygen plasma (25 min) to increase the ITO work function and thereby reduce the barrier for hole injection.<sup>12</sup>

Before the deposition of PVK, an aqueous dispersion of poly(3,4-ethylenedioxythiophene) (PEDOT)–polystyrenesulfonate (PSS) obtained from HC-Starck (Leverkusen, Germany) was spin-cast onto the clean substrates (Fig. 1). The 0.2  $\mu\text{m}$  nylon-filtered PEDOT–PSS had a 1 : 20 weight ratio of PEDOT to PSS. A 50-nm film was spin-cast with 400  $\mu\text{L}$  of solution at 4000 rpm for 30 s; it was then baked in a vacuum oven (0.03 atm) at 150°C for 4 h. PEDOT–PSS is commonly used as a hole injection/transport layer for organic optoelectronic devices.<sup>13</sup> PVK films were then spin-cast on top of the PEDOT–PSS layer and heated in the vacuum oven (0.03 atm) at 60°C for 2 h. Despite this vacuum heat treatment, the solvent (chlorobenzene) remained in the films, as is discussed later.

After vacuum baking, some PVK films were further processed in the absence or presence of an electric field. A voltage of 3 kV of direct current was applied between two parallel metal plates placed 0.5 cm apart; this produced an electric field of 6000 V/cm (0.6 V/ $\mu\text{m}$ ). To prevent arcing due to the breakdown of air, a polyimide film was placed on the bottom plates. For redissolution of the PVK, substrates were placed on the grounded bottom electrode, and

150  $\mu\text{L}$  of chlorobenzene was placed on the spin-cast film. The redissolved film was dried (solvent-evaporated) in an ambient atmosphere without or with the electric field until the solvated droplet disappeared (from 2 h to several hours). These films were then baked again in the vacuum oven (0.03 atm and 60°C) for 2 h.

Metal contacts were thermally evaporated onto the glass/ITO/PEDOT : PSS/PVK samples in a chamber that was evacuated with a mechanical pump and a cryopump to about  $5 \times 10^{-6}$  Torr. Calcium (5 nm) and aluminum (200 nm) films were sequentially deposited at rates of 0.5 and 2 nm/s, respectively. After deposition, the layered structures were dusted with nitrogen and then encapsulated with Loctite™ Extratime 60 epoxy both for mechanical protection and to restrict the access of oxygen and water to the calcium layer. A corner of the device was left unencapsulated to contact the ITO electrode. The finished device structure is shown in Figure 2. All data were collected from the center of the PVK film.

*I*–*V* data were collected to determine the short-circuit current ( $J_{\text{SC}}$ ), the open-circuit voltage ( $V_{\text{OC}}$ ), the power conversion efficiency ( $\eta_p$ ), and the internal quantum efficiency (IQE) of the device.<sup>14</sup>  $J_{\text{SC}}$  is the current at 0 V, whereas the  $V_{\text{OC}}$  is the voltage at zero current. PCE is the ratio between the maximum output device power and the illumination power (expressed as a percentage), and IQE is the number of electrons per absorbed photon (fractional units of electrons per photon).

For illuminated *I*–*V* data, light from an unfiltered Ocean Optics (Dunedin, FL) DH-2000 deuterium tungsten halogen light source was piped through a fiber optic cable onto the sample, and the illumination power was 3.73 mW/cm<sup>2</sup>. A shielded two-point probe configuration was used to collect *I*–*V* data with a Keithley (Cleveland, OH) 238 source controlled by a custom Labview program. Multiple data sets were collected and averaged, and the error was estimated to be less than 10%.

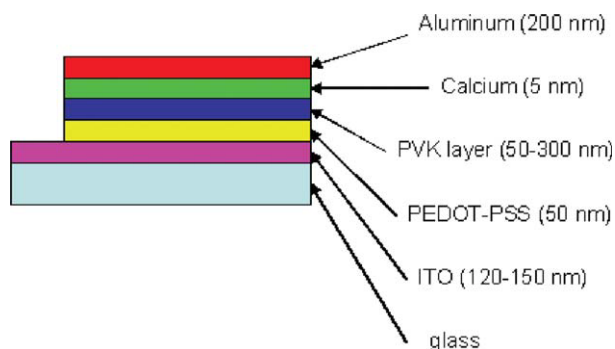


**Figure 2** PV device structure without an epoxy encapsulation layer. [Color figure can be viewed in the online issue, which is available at [www.interscience.wiley.com](http://www.interscience.wiley.com).]

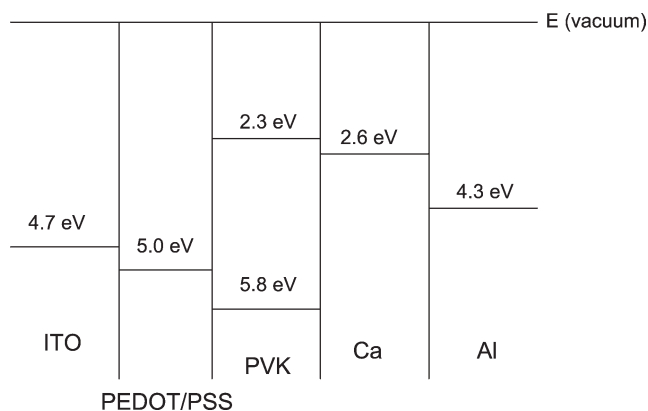


**Figure 3** Energy diagram for the materials used in this study. Energy levels are referenced to the vacuum level ( $E=0$ ).

## RESULTS

An energy band diagram of the glass/ITO/PEDOT : PSS/PVK/Ca/Al multilayered device is shown in Figure 3, where the Fermi energy levels relative to vacuum are shown for ITO, Ca, and Al, and the highest occupied molecular orbital and lowest unoccupied molecular orbital levels are shown for PEDOT-PSS and PVK. The absorption coefficient ( $\alpha$ ) over  $280 \text{ nm} < \text{Wavelength } (\lambda) < 360 \text{ nm}$  for PVK (see Fig. 4) was determined from the amount of light transmitted through PVK films of various thicknesses.  $\alpha$  was near zero for  $\lambda > 360 \text{ nm}$ .

The  $I$ - $V$  data for a device containing a PVK active layer from a 10 mg/mL solution and measured either in the dark or under illumination are shown in Figure 5. The  $\eta_p$  of  $2.9 \times 10^{-5} \%$  fell within the range of  $9.0 \times 10^{-6}$  to  $6.8 \times 10^{-5} \%$  reported by others for single-layer PVK-based devices.<sup>15</sup> The low conversion efficiencies reinforced the conclusion that

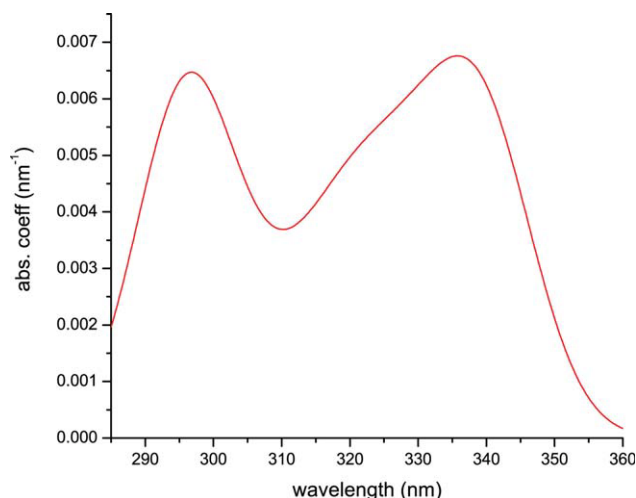


**Figure 4**  $\alpha$ 's versus  $\lambda$  for the PVK thin films. [Color figure can be viewed in the online issue, which is available at [www.interscience.wiley.com](http://www.interscience.wiley.com).]

single PVK layer devices are not viable for practical organic PV cells. However, PVK is appropriate for studying the effects of solution processing on the PV response and molecular configuration. Because the 10 mg/mL films did not exhibit any changes in the molecular configuration upon redissolution,<sup>16</sup>  $I$ - $V$  data were only collected from the spincoated-only condition of these films, which were about 50 nm thick. All of the electrical data were taken from the center of the electrode to prevent errors due to variations in the film thickness ( $t$ ) near the edge of the substrate. The estimated error in the data ( $\pm 10\%$ ) was less than the effects of the molecular configuration on the PV properties.

It is known that the PV mechanism in organic devices is dependent on exciton creation and diffusion to an interfacial barrier where the charges separate.<sup>17</sup> After creation, the exciton travels an average distance, called the *diffusion length*, before annihilation by either radiative or nonradiative events. Typical diffusion lengths are on the order of 10–20 nm for organic materials.<sup>17</sup> Thus, the 10 mg/mL  $t$  ( $\sim 50 \text{ nm}$ ) was two to five times greater than the typical exciton diffusion length ( $L$ ) for polymers. For the probability to be high that the exciton will reach the electrode/polymer interfacial dissociation sites,  $t$  should be less than twice  $L$  so that excitons created in the middle of the layer will be within a diffusion length of the dissociation site. Devices with a polymer film thicker than 200 nm (created by either a slow spincoated speed or high solution concentration) showed no PV response. This was attributed to the fact that, in PVK layers much thicker than the diffusion length, nearly all of the excitons were lost to radiative (i.e., luminescence) or nonradiative (i.e.,

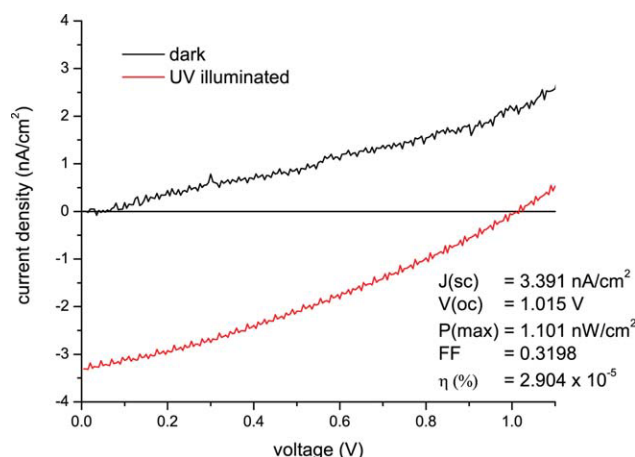


**Figure 5**  $I$ - $V$  data for the PVK-based PV device spincoated from 10 mg/mL of PVK in chlorobenzene. The total currents could be calculated by multiplication by the device area, which was  $0.049 \text{ cm}^2$ . FF, fill factor. [Color figure can be viewed in the online issue, which is available at [www.interscience.wiley.com](http://www.interscience.wiley.com).]

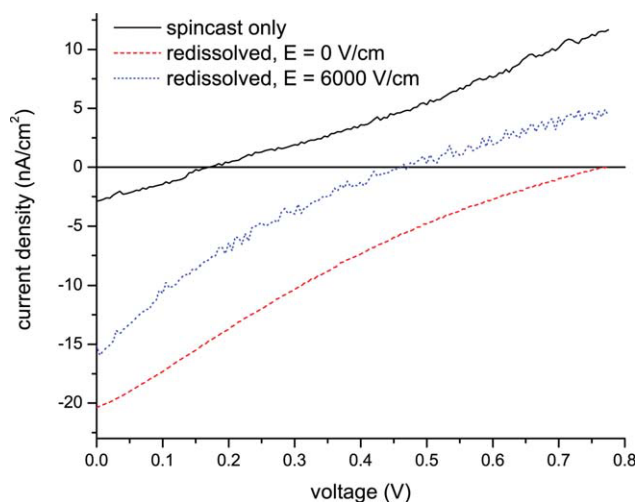


**Figure 6** Illuminated  $I$ - $V$  data for the PVK-based PV device processed from a 50 mg/mL solution.  $E$ , electric field. [Color figure can be viewed in the online issue, which is available at [www.interscience.wiley.com](http://www.interscience.wiley.com).]

phonon emission) recombination events that did not contribute to the external current. If an exciton diffuses to a dissociation site (i.e., to a PVK/electrode interface) and the charges separate, one of the charges must then travel across the entire thickness of the film to reach the opposite electrode to contribute to the current in the external circuit. The probability of the charge encountering traps or other loss mechanisms increased with increasing  $t$ , which again resulting in a low or no PV response for thick films.

To evaluate the effects of solution processing,  $I$ - $V$  data were collected first for films spincast from a 50 mg/mL solution and second after the films were redissolved and dried in the parallel-plate apparatus (discussed in the Experimental section) without (0 V/cm) and with (6000 V/cm) an applied electric field. Of the three process conditions (see Fig. 6), the spincast-only condition led to the lowest  $J_{SC}$  density ( $J_{SC} = 2.9$  nA/cm<sup>2</sup>),  $V_{OC}$  ( $V_{OC} = 0.17$  V), and maximum power ( $P_{max} = 1.5$  nW/cm<sup>2</sup>); this resulted in the poorest  $\eta_p$  of about  $10^{-6}$  %. In addition, IQE (IQE =  $5.5 \times 10^{-6}$ ) was the lowest for the spincast-only processing conditions.

The parameters calculated from the  $I$ - $V$  data in Figure 6 are summarized in the bar graphs in Figure 7. The error bars represent 10% of the value reported for each parameter and processing condition. When the film was redissolved and dried under ambient conditions without the electric field, all factors (i.e.,  $J_{SC}$ ,  $V_{OC}$ ,  $P_{max}$ ,  $\eta_p$ , and IQE), except for the fill factor (FF), increased relative to the control (spincast-only) films. The fill factor remained the same for all process conditions ( $\sim 0.19$  for 50 mg/mL films).  $\eta_p$  increased by an order of magnitude by redissolution

and 0 V/cm ( $4.0 \times 10^{-6}$  to  $8.4 \times 10^{-5}$  %).  $P_{max}$  and IQE increased by a factor of 20 and two orders of magnitude ( $0.15$  to  $3.1$  nW/cm<sup>2</sup> and  $5.5 \times 10^{-6}$  to  $8.7 \times 10^{-4}$  electron/photon), respectively. When the film was redissolved and dried under a 6000 V/cm electric field,  $J_{SC}$ ,  $V_{OC}$ ,  $P_{max}$ , and  $\eta_p$  were lower than the redissolution, 0 V/cm processed film values. In contrast, IQE increased from  $8.7 \times 10^{-5}$  (0 v/cm) to  $1.1 \times 10^{-4}$  electron/photon (6000 V/cm), partially because of the difference in  $t$  between each of the three processing conditions. The PVK material was pushed away from the center and toward the edges during redissolution, which caused the  $t$  at the center of the substrate to decrease. The center  $t$  values cast from the 50 mg/mL solution were 200, 66, and 38 nm for the spincast-only film, the redissolved unexposed film (0 V/cm), and the redissolved exposed film (6000 V/cm), respectively. Despite a decrease in  $P_{max}$ , IQE increased for the redissolved exposed films versus the unexposed films because the number of photons absorbed by the 6000 V/cm film was less than the 0 V/cm condition because of a smaller thickness.

## DISCUSSION

As pointed out previously, the PV mechanism in a PVK organic devices is dependent on (1) absorption of a photon that creates an exciton, (2) diffusion of the exciton to a dissociation site (e.g., the PVK/electrode interface), (3) transfer of the electron from the dissociated exciton to the electrode, and (4) transport of the separated hole through the PVK and collection at the opposite electrode.<sup>17</sup> These four processes affected the IQE as follows<sup>18</sup>:

$$\text{IQE} = \eta_A \eta_{ED} \eta_{CT} \eta_{CC} \quad (1)$$

where  $\eta_A$  is the efficiency for absorption,  $\eta_{ED}$  is the efficiency for exciton diffusion,  $\eta_{CT}$  is the efficiency for charge transfer, and  $\eta_{CC}$  is the efficiency for charge collection. A higher IQE indicated that a larger fraction of absorbed photons resulted in electrons flowing in the external circuit. The absorption and the exciton diffusion efficiencies may be written as<sup>18</sup>

$$\eta_A = (1 - e^{-\alpha t}) \quad (2)$$

$$\eta_{ED} = e^{-t/L} \quad (3)$$

Excitons that are created at distances more than  $L$  away from sites at which they can dissociate are likely to be annihilated before they reach these sites. Therefore, for  $t \gg L$ ,  $\eta_{ED}$  became small. However, for thin films where  $t \ll 1/\alpha$ ,  $\eta_A$  became very small. From Eq. (2), it is evident that a greater thickness will result in higher  $\eta_A$  values but also in lower  $\eta_{ED}$



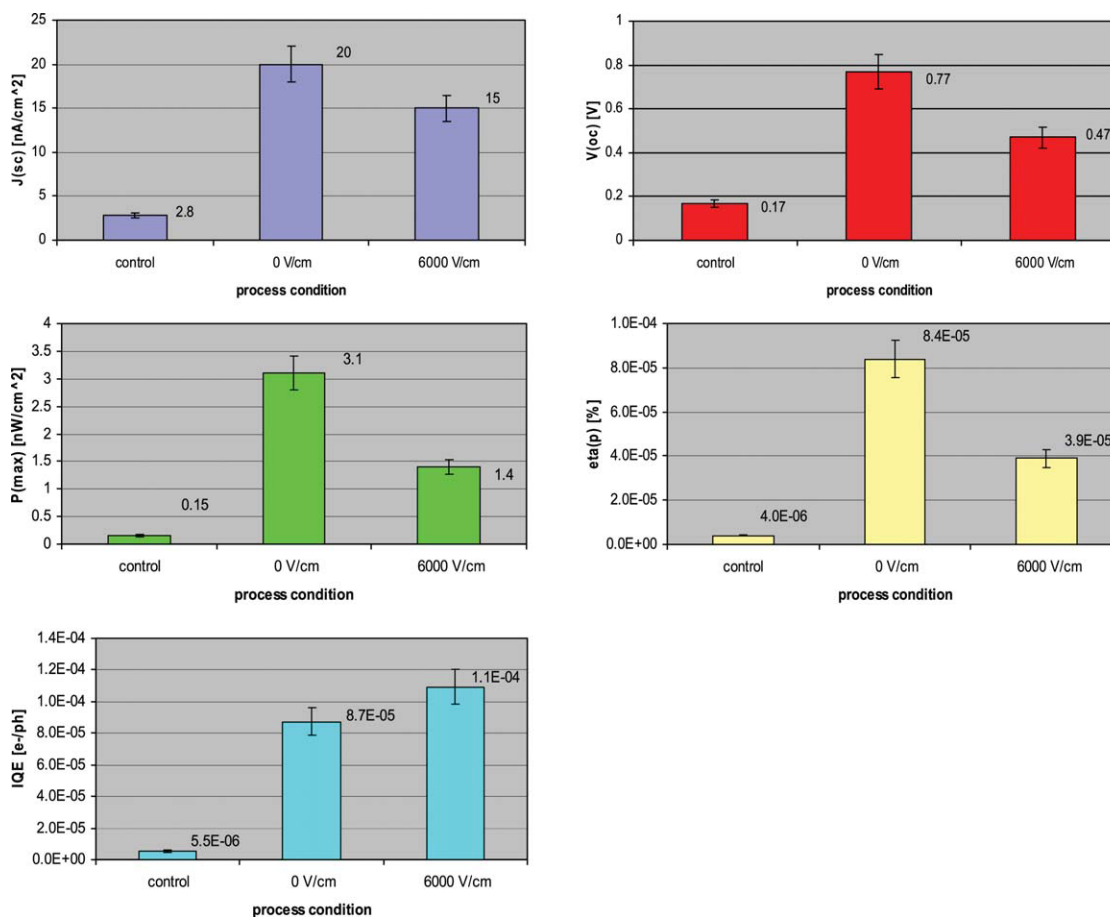


**Figure 7** Values of  $J_{sc}$ ,  $V_{oc}$ ,  $P_{max}$ ,  $\eta_p$ , and IQE calculated from the  $I$ - $V$  data for each of the processing conditions [spin-cast only from 50 mg/mL solutions and redissolved PVK dried without (0 V/cm) and with (6000 V/cm) an electric field]. The error bars represent 10% of the value. The control refers to the spin-cast-only processing. [Color figure can be viewed in the online issue, which is available at [www.interscience.wiley.com](http://www.interscience.wiley.com).]

values, with the assumption that dissociation occurs predominantly at the electrode/polymer interfaces. To maximize the product of  $\eta_A$  and  $\eta_{ED}$ ,  $t$  should be about  $nL$ , where  $n$  is a small number ( $\sim 2$ ). The introduction of dispersed heterojunctions<sup>2,19,20</sup> can increase both the absorption and exciton diffusion efficiencies, but dispersed heterojunctions were not used in this experiment.

For the single-layer device configuration used in this research, the exciton dissociation sites were located at the Ca/PVK and/or PEDOT:PSS/PVK interfaces. In the single-layer configuration, a reasonable value of  $\eta_{ED}$  was achieved for a thickness of about  $2L$  because, at this thickness, an exciton dissociation site was at a distance no more than  $L$  from where the exciton originated. For polymer films processed by solution, the product of  $\alpha L$  is typically 0.1–0.2.<sup>18</sup> The use of these values for the product and an  $\alpha$  equal to about  $0.007 \text{ nm}^{-1}$  (see Fig. 4) resulted in a calculated diffusion length of about 15–30 nm for PVK, with the assumption that  $\alpha$  and  $L$  were unaffected by the redissolution process.

The values of  $\eta_{CT}$  and  $\eta_{CC}$  reflect the probability that the exciton will be separated at a dissociation site and that the separated charges will reach the appropriate electrodes. Because the same electrode materials were used for all devices, it was reasonable to assume that the interfaces remained constant and, therefore, that  $\eta_{CT}$  was the same for all devices. In contrast,  $\eta_{CC}$  was dependent on the charge transport properties of the polymer thin film. In an amorphous material such as solution-processed atactic PVK, where traps originating from structural irregularities are abundant, charges are more likely to encounter traps as their travel distance increases.  $\eta_{CC}$ 's should therefore be smaller for thicker films. As reported previously, the thickness of the center of the PVK film decreased when the spin-cast films were redissolved with solvent. For a 50 mg/mL solution of PVK in chlorobenzene, a spin-cast film resulted in a 200 nm thick film. Upon redissolution of the film with chlorobenzene solvent and subsequent drying under ambient conditions without an electric field, the center thickness decreased to 66

nm. When an electric field was applied during the drying process, the thickness was reduced further to 38 nm. Thus, the lower  $J_{SC}$  from the spin-cast-only film (Fig. 6) was a consequence of the large (200 nm)  $t$ . Because  $L$  was about 15–30 nm, photons absorbed in the interior of the film created excitons at distances too great to reach the PVK/electrode interface before annihilation. This resulted in a low IQE value of  $10^{-6}$  electrons/photon.

For those excitons that reached the interface and were successfully separated, the hole must have moved through the amorphous network of conjugated bonds to the ITO/PEDOT-PSS interface and been collected. The large spin-cast-only  $t$  increased the probability that the transported holes would encounter traps; this led to radiative or nonradiative loss of the carrier and, consequently, to a lower  $\eta_{CC}$ . A larger  $J_{SC}$  was exhibited by the 0 V/cm redissolved condition ( $t = 66$  nm) compared to the spin-cast-only film ( $t = 200$  nm; see Fig. 6) because the separated holes had a shorter distance to travel to reach the opposite electrode. Because the thickness approached the condition of  $t \approx 2L$  ( $L \approx 30$  nm) for the redissolved films, a higher percentage of excitons reached the dissociation sites. This ensured that excitons created anywhere in the layer were less than a diffusion length away from the dissociation site (i.e., the polymer interface).

As discussed earlier,  $J_{SC}$  for the 6000 V/cm redissolved 50 mg/mL film was less than that of the 0 V/cm redissolved film, whereas the IQE value (0 V/cm:  $8.7 \times 10^{-5}$  and 6000 V/cm:  $1.0 \times 10^{-4}$ ) was higher. The thickness of the 6000 V/cm film ( $t = 38$  nm) was approximately equal to the diffusion length ( $\sim 30$  nm); therefore, the exciton diffusion efficiency was high, whereas the photon absorption was less (lower  $\eta_A$ ). A PVK thickness of 38 nm would be expected to result in a smaller  $J_{SC}$  and a larger IQE (i.e., a larger number of electrons per absorbed photons). To check this explanation, the values obtained for IQE,  $\eta_A$ , and  $\eta_{ED}$  were used to calculate the ratio of  $\eta_{CC}$  without and with the electric field, i.e., the ratio of  $\eta_{CC}(0$  V/cm) to  $\eta_{CC}(6000$  V/cm). When Eq. (1) is rearranged,  $\eta_{CC}$  can be expressed as

$$\eta_{CC} = \text{IQE}/(\eta_A \eta_{ED} \eta_{CT}) \quad (4)$$

and  $\eta_{CC}$  ratio of the 0 and 6000 V/cm devices is

$$\eta_{CC}(0)/\eta_{CC}(6000) = (\text{IQE}/\eta_A \eta_{ED} \eta_{CT})_0 \times (\eta_A \eta_{ED} \eta_{CT}/\text{IQE})_{6000} \quad (5)$$

Because we assumed that charge transfer at the electrode/PVK interface was the same for both processing conditions,  $\eta_{CT}$  canceled in Eq. (5). From the

$I$ - $V$  data shown in Figure 6, the data used to calculate the  $\eta_{CC}$  ratio are listed in Table I, and the ratio  $\eta_{CC}(0$  V/cm)/ $\eta_{CC}(6000$  V/cm) was 1.26, which showed that charge collection was more efficient for the thicker 0 V/cm film than for the thinner 6000 V/cm film. This ratio contradicted the previous speculation that thicker films should result in smaller  $\eta_{CC}$  values, but this speculation was based on the assumption that all materials had the same structural features. These ratio data suggest that structural modifications during solution processing affected the charge transport properties and, thus,  $\eta_{CC}$ .

In another study,<sup>16,21</sup> the alignment of adjacent conducting carbazole units in PVK was measured with photoluminescence for the same processing conditions that were used in this study. Photoluminescence in PVK originates from two excimer states, which are described by specific geometric configurations of adjacent carbazole groups as being either partially eclipsed (P) or fully eclipsed (F). When the spin-cast film was redissolved and dried under ambient conditions without an electric field, the P excimer was favored over the F excimer.<sup>16</sup> The P excimer was favored in solution; therefore, reintroduction of the solvent into the film (during the redissolution process) would be expected to increase the number of P excimers. The data presented in this study suggest a correlation between the relative concentration of the P and F excimers and  $\eta_{CC}$ . The 50 mg/mL 0 V/cm films contained greater amounts of P excimer than did the 6000 V/cm films, and they exhibited better charge transport properties, as indicated by an increased  $\eta_{CC}$ . From our previous study, we concluded that the population of the P excimer was related to the amount of residual solvent in the film.<sup>16</sup> Despite vacuum baking (at 0.03 atm and 60°C for 2 h) after the redissolution step, some chlorobenzene solvent remained in the film on the basis of detection by Fourier transform infrared spectroscopy of a C-Cl stretching frequency. We speculated that more residual solvent in the 0 V/cm films favored a higher population of P excimer versus a 6000 V/cm film.<sup>16</sup> Residual chlorobenzene solvent, which has a conjugated structure and is conductive, presumably acted as a conductive bridge

TABLE I  
Data Used to Calculate the  $\eta_{CC}$  Ratio

Figure of merit	Redissolved (0 V/cm)	Redissolved (6000 V/cm)
IQE (electrons/photon)	$8.74 \times 10^{-5}$	$1.09 \times 10^{-4}$
$\eta_A$	0.245	0.152
$\eta_{ED}$	0.111	0.281
$\eta_{CC}$ (in units of $\eta_{CT}$ )	$3.21 \times 10^{-3}$	$2.55 \times 10^{-3}$

between carbazole units, which could facilitate charge transport.

### CONCLUSIONS

Illuminated  $I$ - $V$  data were collected from glass/ITO/PEDOT-PSS/PVK/Ca/Al simple single-layer devices with three different PVK processing conditions, spincast-only or spincast, and redissolved in chlorobenzene followed by drying without (0 V/cm) or with an electric field (6000 V/cm). Devices made from a 50 mg/mL solution concentration produced spincast-only films with thicknesses of 200 nm, that is, much larger than the exciton diffusion distances (15–30 nm); this resulted in reduced exciton dissociation and, therefore, reduced  $\eta_{CC}$ . The films were much thinner after redissolution and drying either without (66 nm) or with (38 nm) an electric field, and higher IQEs and larger  $J_{SC}$ s were observed. The small thickness of the redissolved 6000 V/cm film increased the exciton diffusion efficiency, but the photon  $\eta_A$  decreased faster; this resulted in fewer excitons and, therefore, lower  $J_{SC}$ . On the basis of the IQE, photon absorption, and exciton diffusion data,  $\eta_{CC}$  was greater for the redissolved thicker 0 V/cm film versus the thinner 6000 V/cm films. This was attributed, on the basis of photoluminescence data, to a greater relative population of partially overlapped adjacent carbazole groups in the 0 V/cm PVK films. We speculated that residual solvent in the film stabilized this overlapped structure and led to the improved charge transport properties.

The authors gratefully acknowledge helpful discussions with S. S. Li, J. Reynolds, K. Schanze, and A. Brennan.

### References

1. O'Regan, B.; Grätzel, M. *Nature* 1991, 353, 737.
2. Yu, G.; Gao, J.; Hummelen, J. C.; Wudl, F.; Heeger, A. J. *Science* 1995, 270, 1789.
3. Halls, J. J. M.; Walsh, C. A.; Greenham, N. C.; Marseglia, E. A.; Friend, R. H.; Moratti, Holmes, A. B. *Nature*, 1995, 376, 498.
4. Shaheen, S. E.; Brabec, C. J.; Sariciftci, N. S.; Padinger, F.; Fromherz, T.; Hummelen, J. C. *Appl Phys Lett* 2001, 78, 841.
5. Kruger, J.; Plass, R.; Cevey, L.; Piccirelli, M.; Grätzel, M.; Bach, U. *Appl Phys Lett* 2001, 79, 2085.
6. Mallinaras, G.; Friend, R. *Phys Today* 2005, 58, 53.
7. Kazmerski, L. L. *J Electron Spectrosc* 2006, 150, 105.
8. National Renewable Energy Laboratory, Table of Photovoltaic Performance. [http://www.pv.unsw.edu.au/eff/Effic.%20Table%20\(Table%201\(V18\).pdf](http://www.pv.unsw.edu.au/eff/Effic.%20Table%20(Table%201(V18).pdf) (accessed January 2005).
9. Park, S. H.; Roy, A.; Beaupré, S.; Cho, S.; Coates, N.; Moon, J. S.; Moses, D.; Leclerc, M.; Lee, K.; Heeger, A. J. *Nat Photonics* 2009, 3, 297.
10. Liang, Y.; Feng, D.; Wu, Y.; Tsai, S. T.; Li, G.; Ray, C.; Yu, L. *J Am Chem Soc* 2009, 131, 7792.
11. Handbook of Conducting Polymers; Skotheim, T. A.; Elsenbaumer, R. L.; Reynolds, J. R., Eds.; Marcel Dekker: New York, 1998.
12. Wu, C. C.; Wu, C. I.; Sturn, J.; Kahn, A. *Appl Phys Lett* 1997, 70, 1348.
13. Koch, N.; Elschner, A.; Schwartz, J.; Kahn, A. *Appl Phys Lett* 2003, 82, 2281.
14. Streetman, B.; Banerjee, S. *Solid State Electronic Devices*, 5th ed.; Prentice Hall: Upper Saddle River, NJ, 2000.
15. Nunzi, J. M. C. R. *Physique* 2002, 3, 531.
16. Chung, P. S.; Holloway, P. H. *J Appl Polym Sci* 2009, 114, 1.
17. Senten, C.; Fiorini, C.; Lorin, A.; Nunzi, J. M.; Raimond, P.; Sicot, L. *Synth Met* 1999, 102, 989.
18. Forrest, S. *MRS Bull* 2005, 30, 28.
19. Peumans, P.; Yakimov, A.; Forrest, S. *J Appl Phys* 2003, 93, 3693.
20. Aernouts, T.; Geens, W.; Poortmans, J.; Heremans, P.; Borgh, S.; Mertens, R. *Thin Solid Films* 2002, 403–404, 297.
21. Chung, P. S. Ph.D. dissertation, University of Florida, 2007.